

# Supplemental Materials

June 21, 2023

This document provides supplemental materials for the manuscript entitled “Coverage Optimization of Robotic Sensor Networks in Non-Convex Environments via Rotary Pointer Partitions” by Chao Zhai, Pengyang Fan and Hehong Zhang, and it is composed of two parts. The first part discusses simulation results on the robustness of rotary pointer partition to disturbances and the removal/insertion of robots, and the second part provides experimental results on the proposed coverage control approach in the robotic platform of Robotarium.

## 1 Robustness to Disturbances

In the traditional Voronoi tessellation based coverage control, the Voronoi partitions are dependent on the positions of robots. In comparison, the proposed rotary pointer partitions are independent of the positions of robots for the fixed neighborhood of robots, which enables to flexibly update the rotary pointers for region partition with the added benefits of equalizing the workload among subregions. Since each robot is equipped with a virtual rotary pointer, the ordering of rotary pointers is dependent on the neighborhood of robots (i.e., the sequence of robots). As a result, the proposed rotary partitions can be implemented reliably if the perturbation of robot positions does not change the neighborhood of robots. In what follows, the robustness of proposed partition approach to disturbances on robots is taken into account.

### 1.1 Mild disturbances on robots

Figure 1 illustrates the change of robot position after the mild disturbance is added on the  $i$ -th robot. Since the  $i$ -th robot still stays in its own subregion after mild disturbances, the neighborhood of robots remains unchanged, thereby ensuring the normal rotary partitions and coverage control. Figure 2 presents the snapshots of multi-robot coverage when the mild disturbances are added on the 3rd and 4th robots (red circles) at time  $t = 20$ s, and the time evolution of workload partition, phase angle and coverage

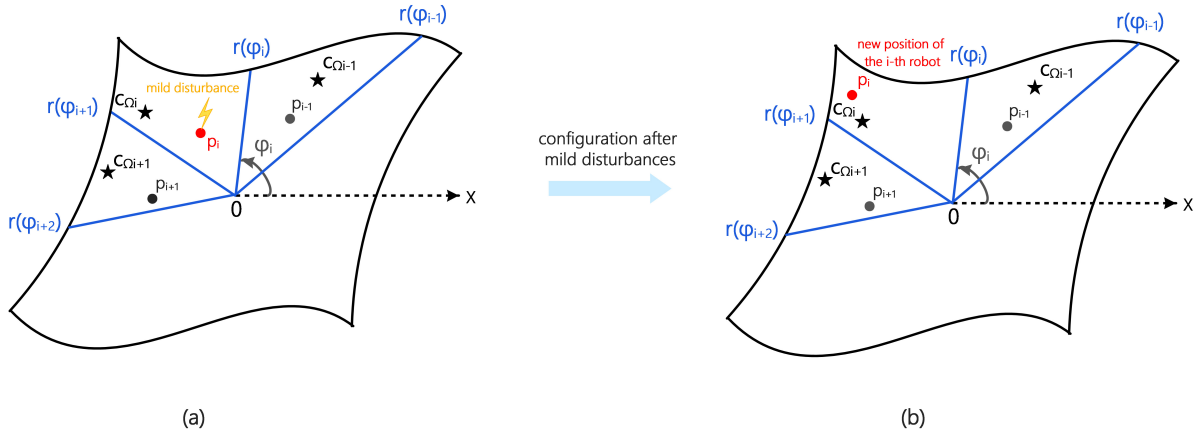


Figure 1: The change of robot positions after adding mild disturbances. The red ball represents the position of the  $i$ -th robot, and the yellow lightning denotes the disturbance that is added on the  $i$ -th robot. The blue segments stand for the rotary pointers, and the black pentagram refers to the centroid of subregion.

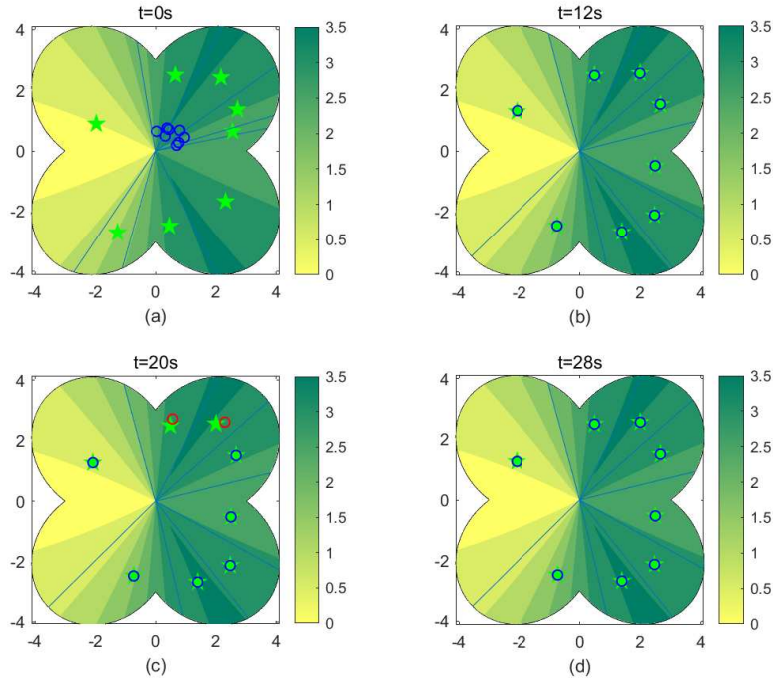


Figure 2: Snapshots of multi-robot coverage with mild disturbances.

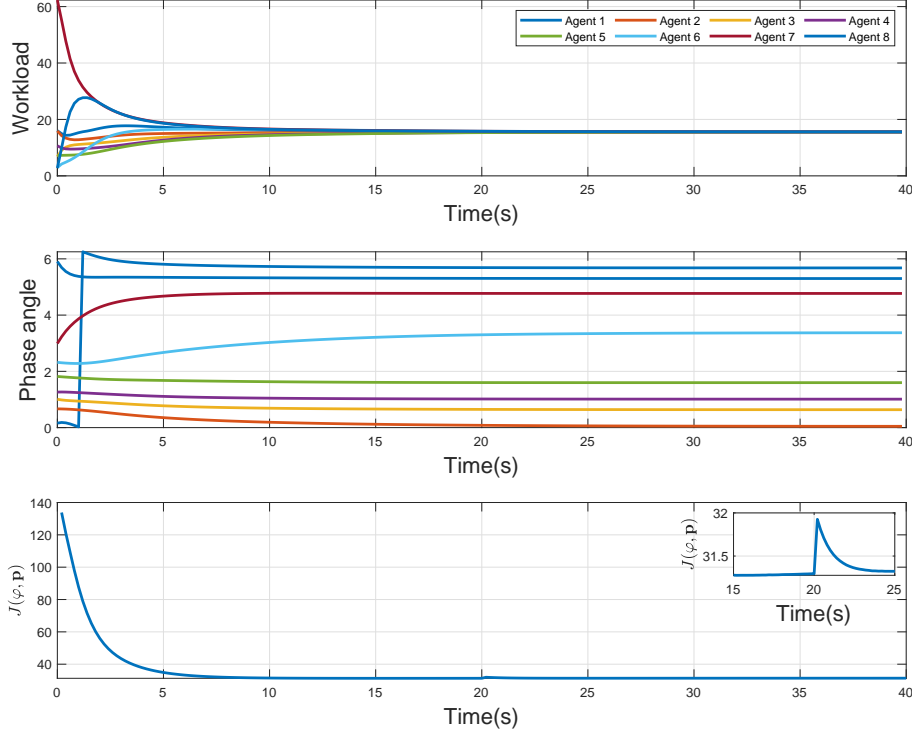


Figure 3: Time evolution of multi-robot coverage with mild disturbances.

cost is shown in Fig. 3. As is observed, the coverage control algorithm still goes well, expect for a tiny perturbation of the coverage cost  $J(\varphi, \mathbf{p})$  at time  $t = 20$ s. This is because the mild disturbances cause the two robots to deviate from the centroid of their respective subregions, which leads to the increase of the coverage cost.

## 1.2 Severe disturbances on robots

If the severe perturbation causes the robot to leave its assigned subregion and changes the neighborhood of robots, the rotary partitions will be redefined and the partition dynamics is implemented according to the updated neighborhood of robots. Figure 4 shows the change of robot positions when severe disturbances are added on the  $i$ -th robot. The severe disturbances cause the  $i$ -th robot to leave its own subregion and also change the neighborhood of robots (e.g., the  $i$ -th robot is no longer the neighbor of the  $(i - 1)$ -th agent after the severe disturbance). Thus, the partition dynamics will be implemented according to the new neighborhood of robots, thereby redefining the rotary partitions to balance the workload and fulfill the coverage mission, although the severe disturbance in the proposed architecture might cause a robot to leave its assigned partition. Figure 5 and Figure 6 present the snapshots and time evolution of multi-

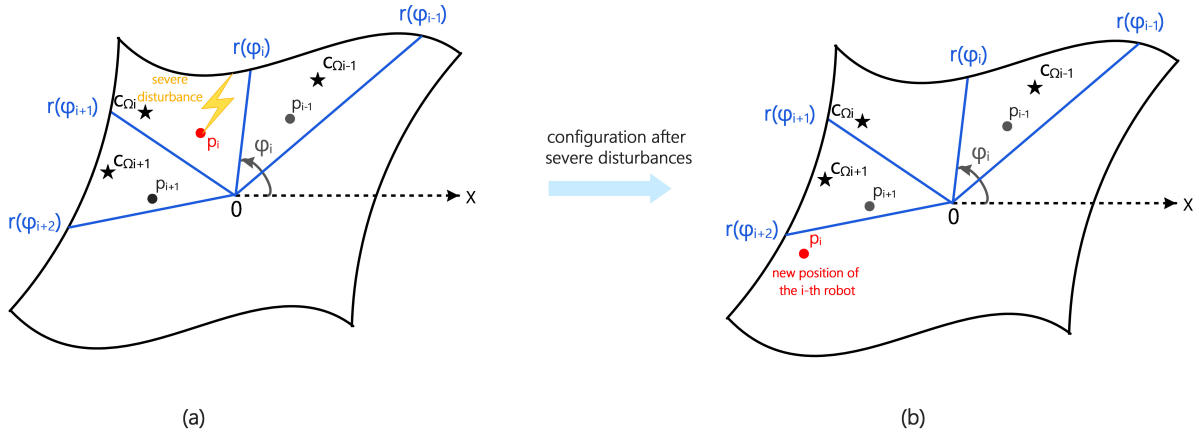


Figure 4: The change of robot positions after adding severe disturbances.

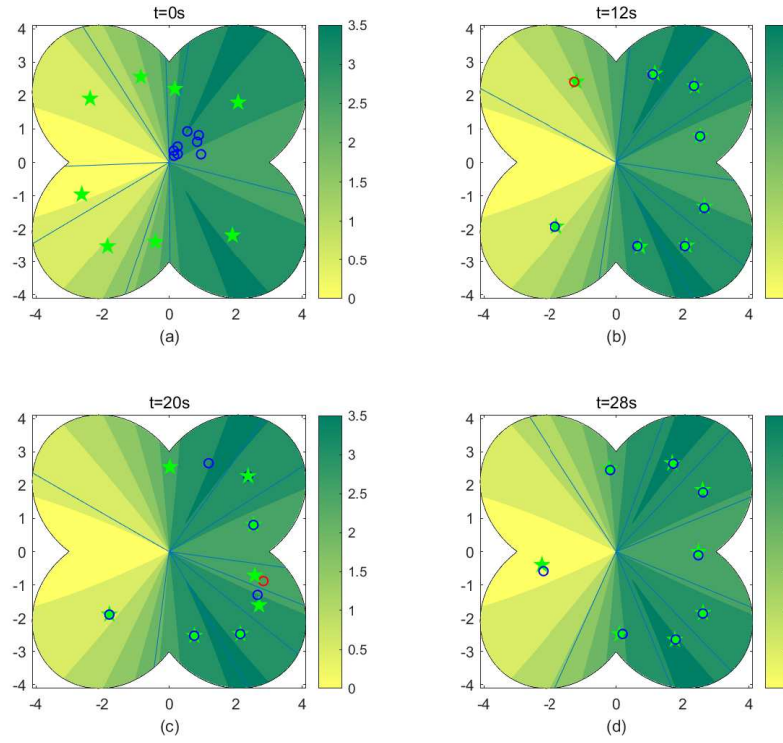


Figure 5: Snapshots of multi-robot coverage with severe disturbance.

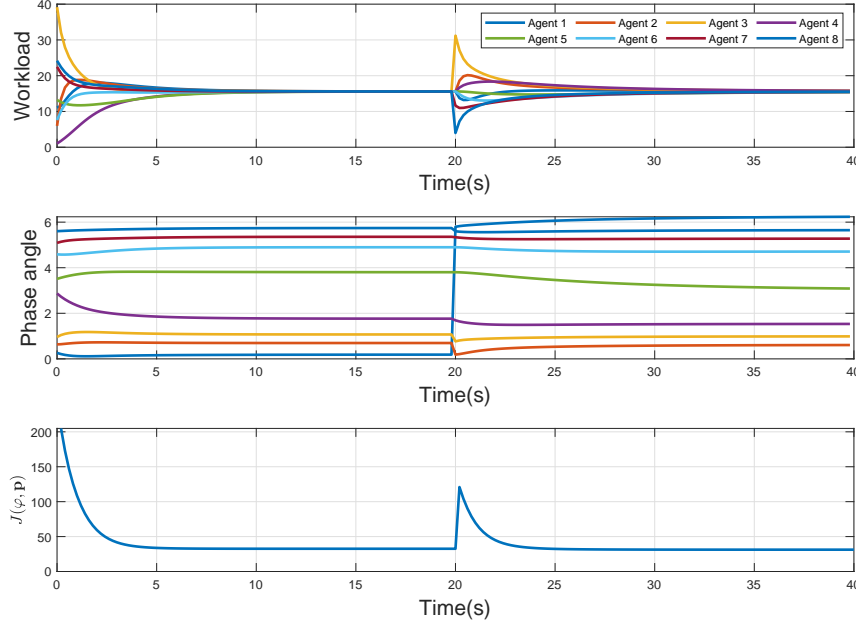


Figure 6: Time evolution of multi-robot coverage with severe disturbance.

robot coverage in the numerical simulation, respectively. A severe disturbance is added on the 3rd robot (red circle) at time  $t = 20$ s, which causes the robot to leave its subregion and consequently change the neighborhood of robots. It is observed that the subregion workload, phase angles and the coverage cost are all perturbed visibly after the severe disturbance. Nevertheless, the coverage control algorithm continues to work, and multi-robot system converges to a new configuration in the end. This implies that the rotary partitions are also robust to disturbances on the robots.

### 1.3 Removal of the robot

The rotary partition approach is also robust to the disturbances such as the removal or insertion of robots. Actually, the removal or insertion of robots may lead to reconstructing the neighborhood and communication topology of multi-robot system, and the rotary partition and region coverage can be fulfilled if the condition  $\lambda_{\min} > 0$  holds. Figure 7 presents four snapshots of multi-robot coverage when one robot (i.e., the 8th robot) is removed at time  $t = 20$ s, and Figure 8 shows the evolution of subregion workload, phase angle of rotary pointers and coverage cost. Note that the communication topology of multi-robot system is a directed ring, and it is still connected with  $\lambda_{\min} > 0$  after the removal of one robot. In addition, the removal of one robot results in the disappearance of its rotary pointer, which may give rise to the increase

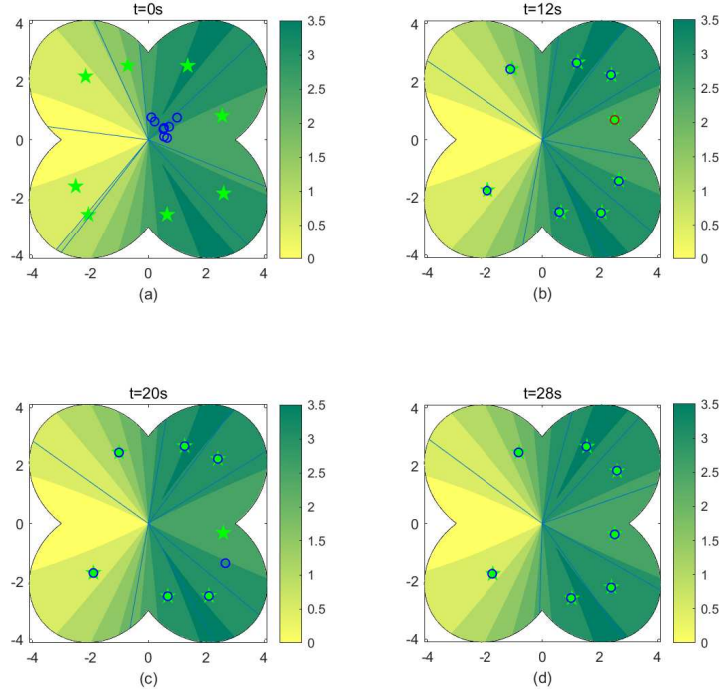


Figure 7: Snapshots of multi-robot coverage with removal of one robot.

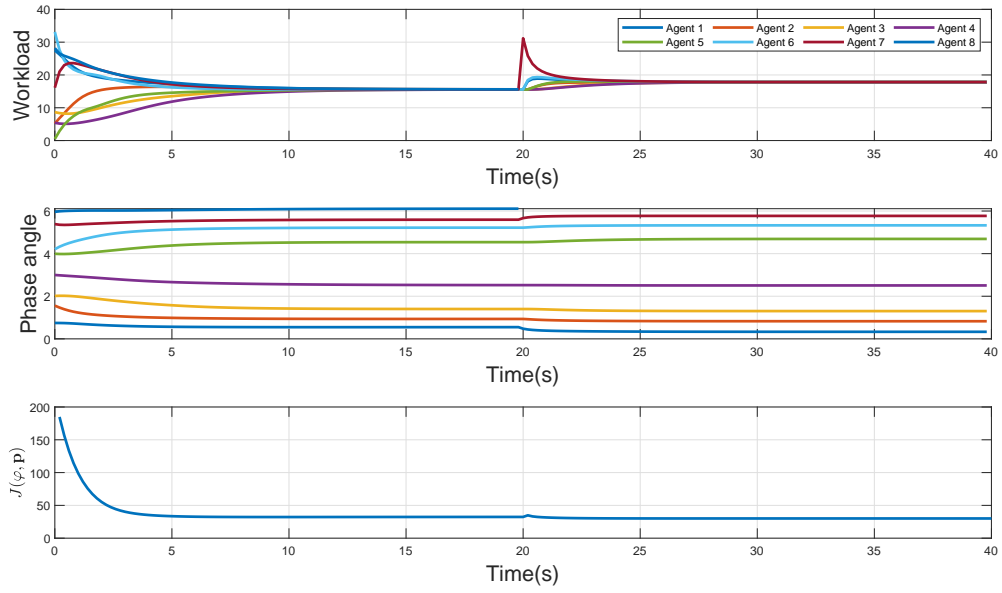


Figure 8: Time evolution of multi-robot coverage with removal of one robot.

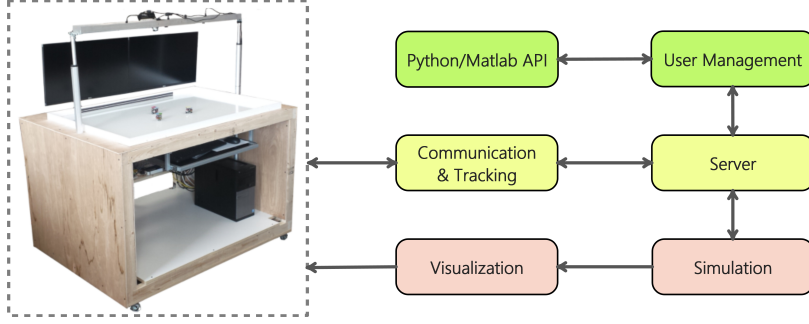


Figure 9: Experimental platform for multi-robot coverage optimization using Robotarium [1].

of workload on the adjacent subregion. As is observed, the workload on the subregion of the 7th robot surges after removing the 8th robot at  $t = 20$ s and then converges to the same value as other subregions. Likewise, although the phase angles of rotary pointers and coverage cost are also disrupted at  $t = 20$ s due to the removal of the robot, they can still converge to the accurate values in the end. For the insertion of robots, multi-robot system is also able to absorb the disturbances and get back to the normal condition.

## 2 Experimental Validation

Experimental validation aims to test the practical feasibility of proposed coverage control algorithm and investigate how control commands drive robots to coordinate their behaviors in practice. Compared with numerical simulations, real robots are adopted with non-holonomic constraints in the experiments, and obstacle avoidance is guaranteed through infrared distance sensing.

### 2.1 Experimental setup

The remote-access experiments are carried out on an open multi-robot platform of Robotarium to validate the proposed coverage algorithm [1], Figure. 9 illustrates the experimental architecture of Robotarium, and the platform is composed of robot hardware (for motion tracking, wireless communication, and virtualization) and remote user machines (for user management, code verification and upload, etc). In the experiment, eight robotic vehicles move in the area of  $3.2m \times 2m$ . The polar equation of coverage region and the workload density function are the same as those in numerical simulations. Likewise, the initial position and orientation of mobile robots and phase angles of rotary pointers are assigned at random. The corresponding experimental video has been uploaded onto the website [2], and each trial lasts for 30s.

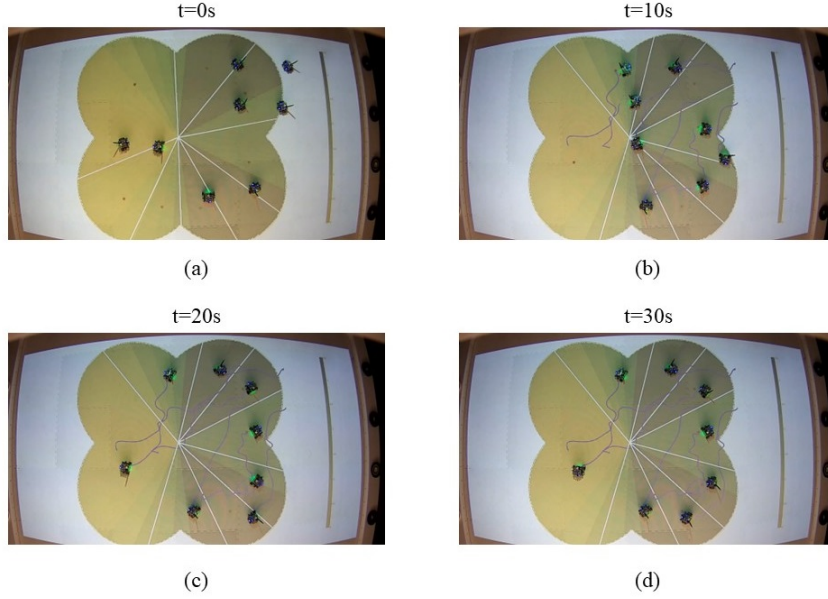


Figure 10: Snapshots of experimental results on region partition, subregion centroids and positions of multi-robot systems in the platform of Robotarium.

## 2.2 Discussions

Figure 10 provides four snapshots on experimental process of multi-robot locational optimization. Therein, the white lines represent the rotary pointers among subregions, and red stars refer to the subregion centroids. In addition, blue lines show the trajectories of robots. The color map indicates the magnitude of workload density, and a darker color implies a higher value of density. As is observed, the rotary pointers among subregions converge to their respective limit values quickly, and they largely keep unchanged after 10s. In comparisons, each robot firstly moves into its own subregion and then gradually arrives at the subregion centroid. The robot trajectories indicate that some robots have to come across the subregions of other robots before entering its own territory. Notably, it takes about 25s to complete the deployment of multi-robot systems for monitoring and tackling random events. The above experimental results demonstrate the efficacy of proposed coverage algorithm in practice. It manages to fulfil the locational optimization task in non-convex environments, and the value of cost function for region coverage is worth 193.41 at the end of experiments. In addition, Figure 11 presents the evolution of coverage cost in the Robotarium experiment. As is observed, the coverage cost in the experiment goes up slightly at the initial time and then gradually declines to the stable value after 15s. The initial non-monotonicity of coverage cost mainly results from the high efficiency of pointer partition and relatively low-speed motion of robots. As a consequence, the distance between the robot and the centroid of its subregion may get



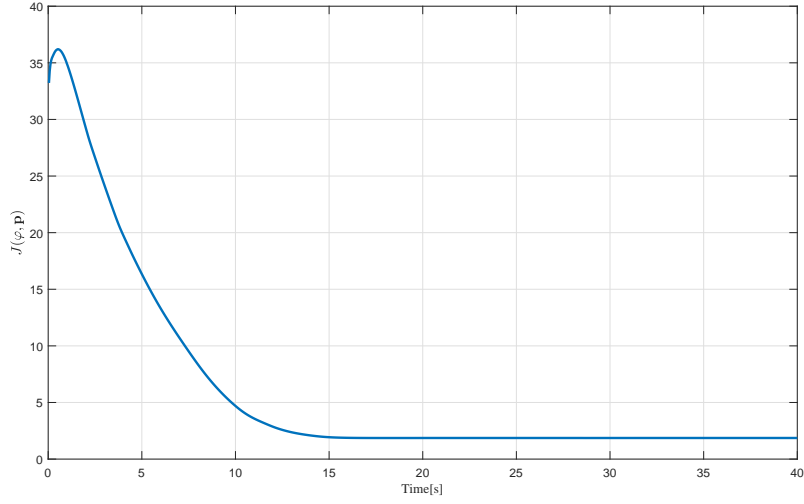


Figure 11: Time evolution of the coverage cost in the Robotarium experiment.

large initially and then gradually decrease after the workload partition is almost completed.

## References

- [1] D. Pickem, E. Squires, and M. Egerstedt, The Robotarium: An open, remote-access, multi-robot laboratory, 2016.
- [2] Experimental video at <https://www.youtube.com/watch?v=0iOaYYtH3t0>.